TITLE:

Cu/Si interface fracture due to fatigue of copper film in nanometer scale

AUTHOR(S):

Sumigawa, Takashi; Murakami, Tadashi; Shishido, Tetsuya; Kitamura, Takayuki

CITATION:

Sumigawa, Takashi ...[et al]. Cu/Si interface fracture due to fatigue of copper film in nanometer scale. Materials Science and Engineering: A 2010, 527(24-25): 6518-6523

ISSUE DATE:

2010-09-25

URL:

http://hdl.handle.net/2433/128866

RIGHT:

© 2010 Elsevier B.V.; この論文は出版社版でありません。引用の際には出版社版をご確認ご利用ください。; This is not the published version. Please cite only the published version.

京都大学学術情報リポジトリ
KURENAI 紅
Kyoto University Research Information Repository

京都大学 KYOTO UNIVERSITY
A Self-archived copy in
Kyoto University Research Information Repository
https://repository.kulib.kyoto-u.ac.jp
京都大学学術情報リポジトリ KURENAI 紅 Kyoto University Research Information Repository

Cu/Si Interface Fracture due to Fatigue of Copper Film in Nanometer Scale

Authors: Takashi Sumigawa[1*], Tadashi Murakami [1], Tetsuya Shishido[1], and Takayuki Kitamura[1]

Affiliations:

1 Department of Mechanical Engineering and Science, Kyoto University, Kyoto 606-8501, Japan

*Corresponding author

Abstract

In order to investigate the fatigue behavior of metals in nanoscale, a cyclic bending experiment is carried out using a nano-specimen. The specimen includes a copper film with a thickness of 20 nm constrained by highly rigid materials, which yields a high strain region with a size of a few nanometers near the interface edge. The specimen broke before the maximum load in the 7th cycle under fatigue (load range of 18 μN). The load-displacement curve shows nonlinear behavior and a distinct hysteresis loop, indicating plasticity in the Cu film. Reverse yielding appearing after the 2nd cycle suggests the development of a cyclic substructure in the Cu film. The cumulative plastic strain in the Cu film at fracture is more than three times larger than that under monotonic loading. These results indicate that the specimen breaks owing to fatigue of the Cu film on the nanoscale.

1. Introduction

In fatigue of bulk metals, irreversible cyclic deformation results in characteristic dislocation structures (vein, ladder-structure, and cell) [1-7]. In particular, the ladder structure and cell cause crack initiation owing to strain localization because they are much softer than the matrix [8-10]. It is well known that these substructures in fatigue have a size on the scale of a few micrometers [1-3].

Micro- or nano-scale components, in general, are fabricated from multi-layered thin films, incorporating a large number of dissimilar interfaces. Near an interface, stress often concentrates owing to the deformation mismatch between dissimilar materials. In particular, strong stress concentration occurs at the interface edge where a dissimilar interface meets the surface [11, 12]. Since the stress-concentration region is proportionally scaled down for shrinkage of component size, the strain-concentration region is a few nanometers or at most a few tens of nanometers in advanced devices.

京都大学 KYOTO UNIVERSITY
A Self-archived copy in
Kyoto University Research Information Repository
https://repository.kulib.kyoto-u.ac.jp
京都大学学術情報リポジトリ KURENAI 紅 Kyoto University Research Information Repository

Thus, the typical fatigue substructures observed in bulk metals cannot form in these nanoscale regimes. Although several researchers [13-15] have explored the fatigue property of nano-films, it is not well understood yet because of experimental difficulty.

Recently, focused ion beam (FIB) processing has enabled fabrication of nanoscale specimens for precise mechanical testing [16, 17]. In addition, a recently developed advanced loading system composed of a piezoelectric actuator and MEMS (Micro electro mechanical systems) load and displacement sensors makes it possible to directly apply a sensitive load to the nanoscale specimen and then measure it [18-21].

In this study, using a nano-specimen incorporating a copper film with a thickness of 20 nm constrained by highly rigid materials, wherein the strain concentrates in a region of a few tens of nanometers, the fatigue behavior is investigated by a cyclic bending experiment.

京都大学 KYOTO UNIVERSITY
A Self-archived copy in
Kyoto University Research Information Repository
https://repository.kulib.kyoto-u.ac.jp
京都大学学術情報リポジトリ KURENAI 紅 Kyoto University Research Information Repository

2. Experiment and experimental procedure

2.1 Material and Specimen

After the native oxide layer on a silicon (Si) substrate is removed by argon ion etching, films of copper (Cu: 20 nm thickness) and silicon nitride (SiN: 500 nm thickness) is continuously deposited by magnetron sputtering at rates of 24 and 10.5 nm/min, respectively. Passivation layers of platinum, carbon, and tungsten are formed on it in order to protect the SiN layer from the subsequent focused ion beam (FIB) processing. A nanometer scale cantilever specimen, shown in the transmission electron microscope (TEM) micrograph in Fig.1(a), is carved out of the multi-layered plate by FIB processing [18, 19]. To avoid the formation of a damaged layer, the surface is finely finished using a weak ion beam (10 pA). The dimensions of the specimens are summarized in Fig.1(b).

2.2 Equipment and Experimental Conditions

A load was applied to the SiN layer away from the Cu film by a diamond pyramid tip, as illustrated in Fig.2. A load sensor, attached to the back of the tip, can directly detect the applied load. The measurement range and accuracy of the load are 0-100 μN and ±0.1 μN, respectively.

The loading apparatus is comprised of a stage driven by a piezo-actuator along with a diamond tip [19-21] installed in a TEM for *in-situ* observations. In this study, the purposes of the TEM observations are to identify the location of the interfaces, to elucidate fracture features, and to accurately measure the specimen deformation. Metallographic observations through the specimen are out of the scope of the present experiment. TEM observations are carried out with an accelerating voltage of 200 kV under a vacuum of 1.5×10^{-5} Pa. The displacement at the end of the arm, δ, (See Fig. 2) is measured using the TEM.

The fatigue (cyclic load) experiment is conducted for Specimen 1 under a constant load range, $\Delta P = P_{max}$-P_{min}, with a load ratio of $P_{min}/P_{max} = 0$ (P_{min}: minimum load, P_{max}: maximum load). The initial load range is 8 μN, which is increased to 9 μN after 100 cycles. This process of 100 cycle fatigue and load increase (1 or 1.5 μN) is repeated until the specimen breaks under $\Delta P = 18$ μN (Fig. 3(a)).

For comparison, the monotonic bending experiment is conducted using Specimen 2 (Fig. 1 (b) and Fig. 3(b)).

京都大学 KYOTO UNIVERSITY
A Self-archived copy in
Kyoto University Research Information Repository
https://repository.kulib.kyoto-u.ac.jp
京都大学学術情報リポジトリ KURENAI 紅 Kyoto University Research Information Repository

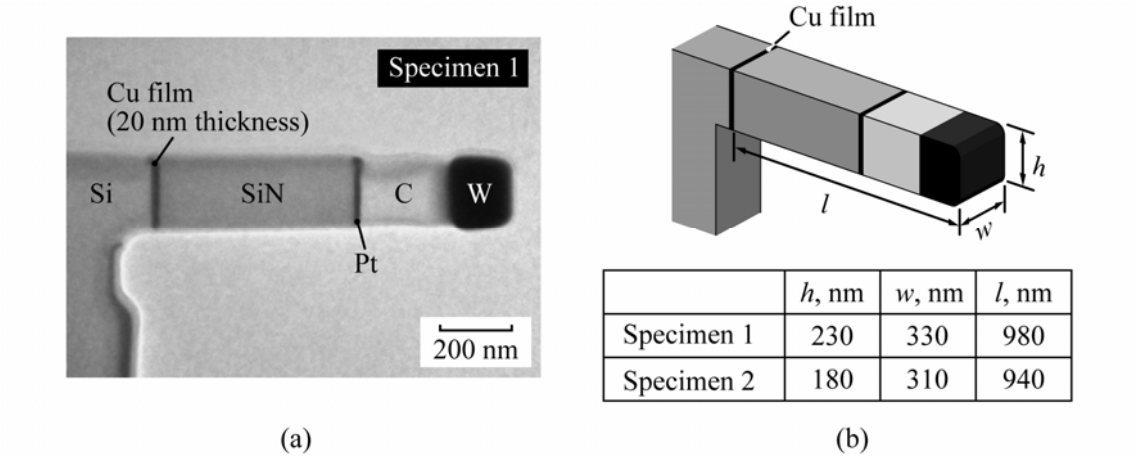

	h, nm	w, nm	l, nm
Specimen 1	230	330	980
Specimen 2	180	310	940

Fig. 1 (a) Nano-cantilever specimen. Transmission electron microscope (TEM) micrograph of a specimen. A 20 nm-thickness Cu thin film is sandwiched between dissimilar materials with high rigidity (Si substrate and SiN layer), and (b) Dimensions of the two specimens used.

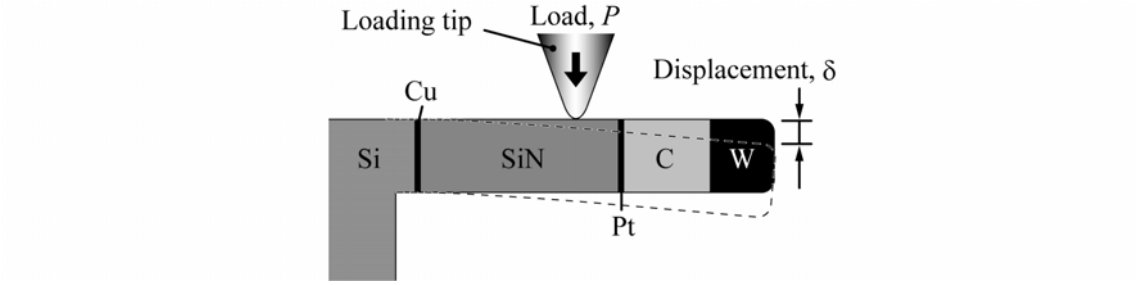

Fig. 2 Loading method. Load is applied to the SiN layer in the cantilever specimen by a loading tip, and the displacement of the arm end, δ, is measured in the TEM.

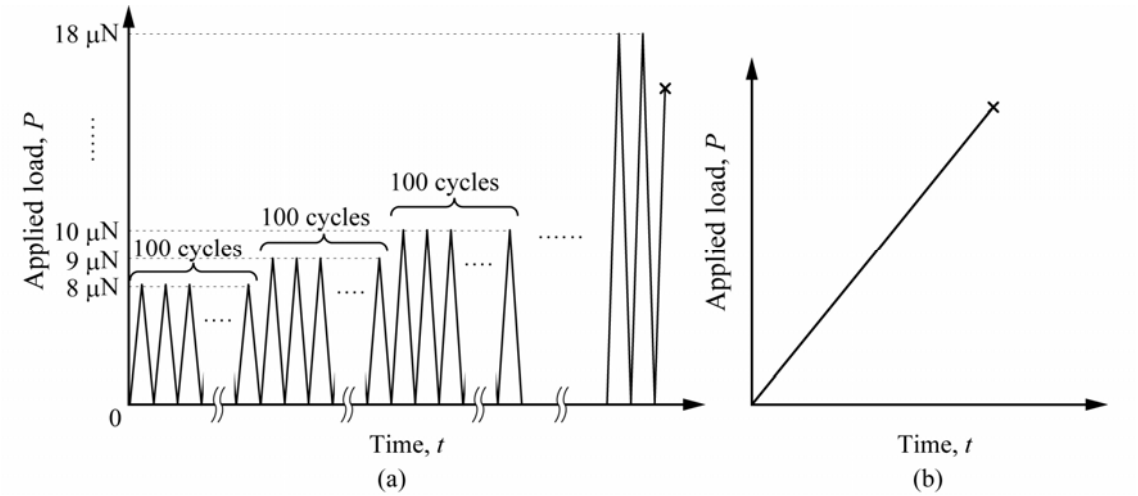

Fig. 3 Schematic illustration of the loading condition: (a) fatigue experiment with a constant load range, and (b) monotonic bending experiment.

京都大学 KYOTO UNIVERSITY
A Self-archived copy in
Kyoto University Research Information Repository
https://repository.kulib.kyoto-u.ac.jp
京都大学学術情報リポジトリ KURENAI 紅 Kyoto University Research Information Repository

2.3 Fatigue region in nano-scale

In order to approximately estimate the fatigue region (high strain region) in Specimen 1, we conducted elastic and elasto-plastic analyses using the finite element method (FEM, Fig. 4(b a)) using the constitutive equation in monotonic loading [21]. The elastic constants used in the analysis are listed in Fig. 4(a) while the elasto-plastic one of the Cu film is in the form:

$$\sigma = \begin{cases} 129000\varepsilon & \text{, for} \quad \sigma \le 765 \ \text{[MPa]} \\ 3316\varepsilon^{0.3} & \text{, for} \quad \sigma \ge 765 \ \text{[MPa]} \end{cases}. \tag{1}$$

The validity of Eq.(1) has been discussed in detail in the previous paper [21].

The result shown in Fig. 4(b) indicates that the strain concentrates in the region of r < 40 nm in both cases, though the magnitude of the strain is different. Deep inside the Cu film, it is hard for the dislocations to move owing to the absence of a free surface and the strong constraint of the highly rigid materials (Si: σ_y > 3.4 GPa [22] and SiN: σ_y > 3.4 GPa [23] ; σ_y is the yield stress) in addition to the low stress level. Hence, the fatigue region expected is about 40 nm × 20 nm × 330 nm in the Cu film as schematically illustrated in Fig.4(c). Although the result is not exact because the constitutive equation is for monotonic deformation, not for cyclic one, it points out that the fatigue region is in the nanometer scale.

京都大学 KYOTO UNIVERSITY
A Self-archived copy in
Kyoto University Research Information Repository
https://repository.kulib.kyoto-u.ac.jp
京都大学学術情報リポジトリ KURENAI 紅 Kyoto University Research Information Repository

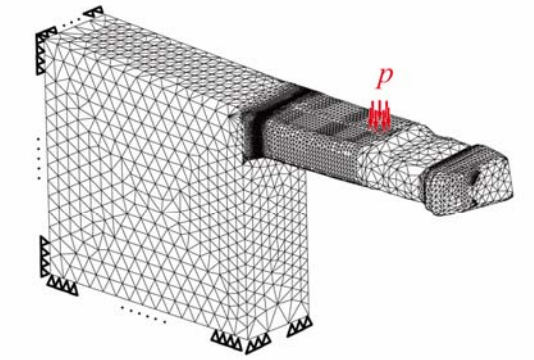

Material	Young's modulus (GPa)	Poisson's ratio
Cu	129	0.34
SiN	197	0.27
Pt	168	0.377
C	10	0.3
W	407	0.17

	C_{11} (GPa)	C_{12} (GPa)	C_{44} (GPa)
Si	167.4	65.23	79.57

(a)

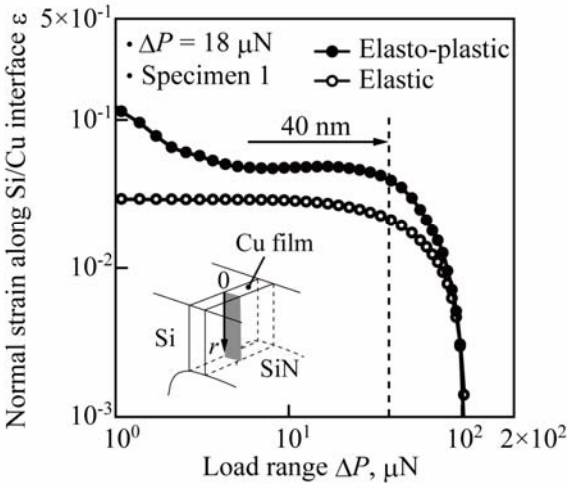

(b)

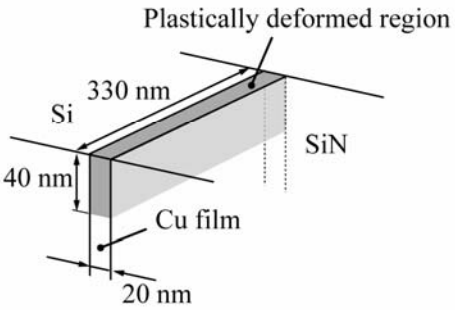

(c)

Fig. 4 (a) Analytical model for elastic and elasto-plastic FEM analyses, (b) strain distributions along the Cu/Si interface near the edge in Specimen 1 under monotonic loading, and (c) fatigue region (plastically deformed region) in the Cu film of Specimen 1.

3. Results and Discussion

3.1 Cyclic deformation

Figure 5 shows TEM micrographs obtained during the 1st cycle under ΔP = 18 μN. The locations of the dissimilar interfaces and the loading point are clearly identified by the experimental system. It also clarifies no slip between the tip and the specimen. Since the arm extension of Pt/C/W gives sufficient magnification of deformation in the loaded section [18-21], specimen elongation on the upper face can be quantitatively measured with sufficient accuracy.

Figure 6 shows the load-displacement (P-δ) curves in the 1st, 2nd, 3rd, and 99th cycles under the initial load range (ΔP = 8 μN). Here, δ is the displacement at the arm end. The linear and reversible behavior in each cycle indicates that the specimen, including the Cu layer, elastically deforms under the cyclic loading. In the figure, the

京都大学 KYOTO UNIVERSITY
A Self-archived copy in
Kyoto University Research Information Repository
https://repository.kulib.kyoto-u.ac.jp
京都大学学術情報リポジトリ KURENAI 紅 Kyoto University Research Information Repository

broken line shows the relation obtained from elastic FEM analysis, wherein the shape of the analytical model is precisely reconstructed on the basis of TEM and SEM observations (See Fig. 4(a)). The fact that the *P*-δ curves experimentally obtained are in close agreement with the analytical one indicates the sufficient accuracy of the experimental device in the measurement of load and displacement. The gradient of the *P*-δ curve does not change until the last cycle. For fatigue experiments, long-term stability of the experimental system is essential. The elastic deformation ensures the reliability of our system in fatigue.

Careful examination of the *P*-δ relation in the 1st and 99th cycles reveals residual displacement, δ', of about 10 nm after the 99^{th} cycle. Considering the measurement precision, this signifies the accumulation of plastic strain in the specimen, though the magnitude of this accumulated strain in each cycle cannot be individually identified. Figure 7 shows δ' in the last cycle under each load range revealing that irreversible (plastic) strain accumulates with the progress of cyclic deformation. In particular, δ' rapidly increases under $\Delta P = 18$ μN.

京都大学
KYOTO UNIVERSITY
A Self-archived copy in
Kyoto University Research Information Repository
https://repository.kulib.kyoto-u.ac.jp
京都大学学術情報リポジトリ
KURENAI 紅
Kyoto University Research Information Repository

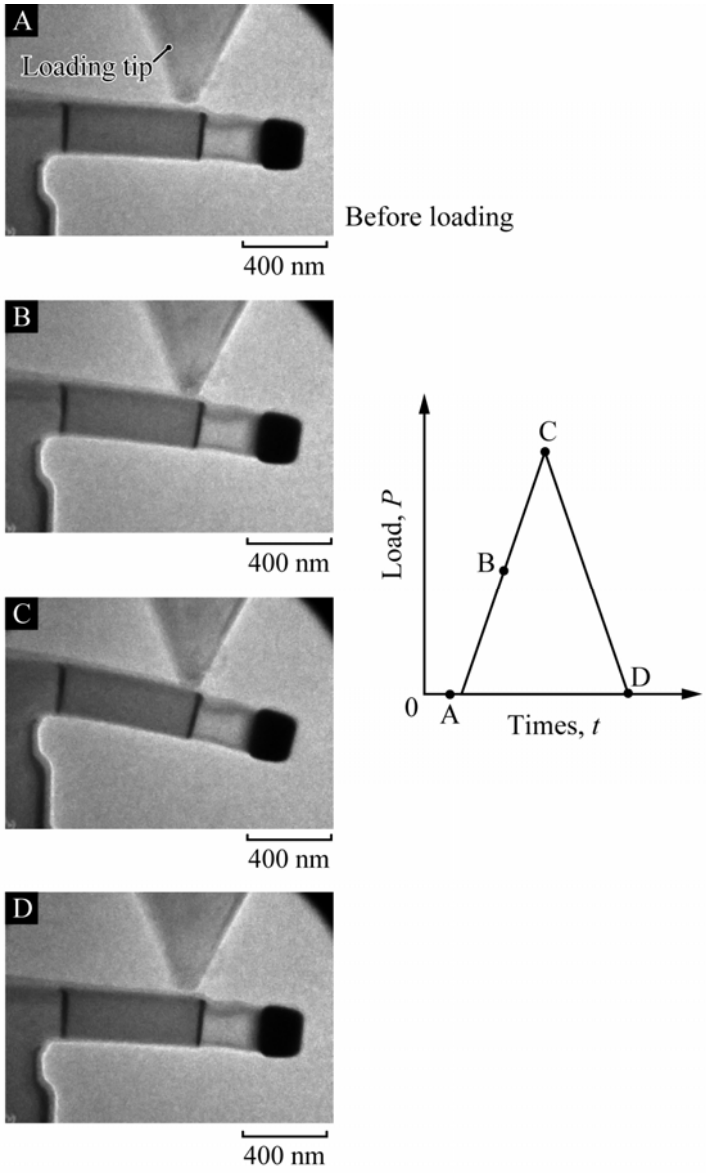

Fig. 5 TEM micrographs in the first cycle under ΔP = 18 μN.

京都大学 KYOTO UNIVERSITY
A Self-archived copy in
Kyoto University Research Information Repository
https://repository.kulib.kyoto-u.ac.jp
京都大学学術情報リポジトリ KURENAI 紅 Kyoto University Research Information Repository

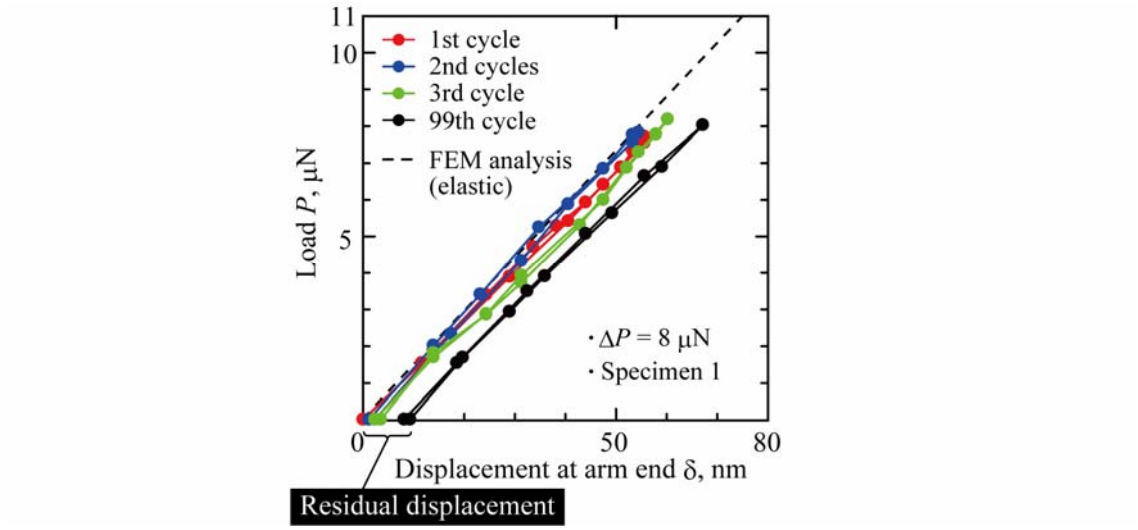

Fig. 6 Load-displacement curves at 1, 2, 3, and 99 cycles under the initial load range (ΔP = 8 μN).

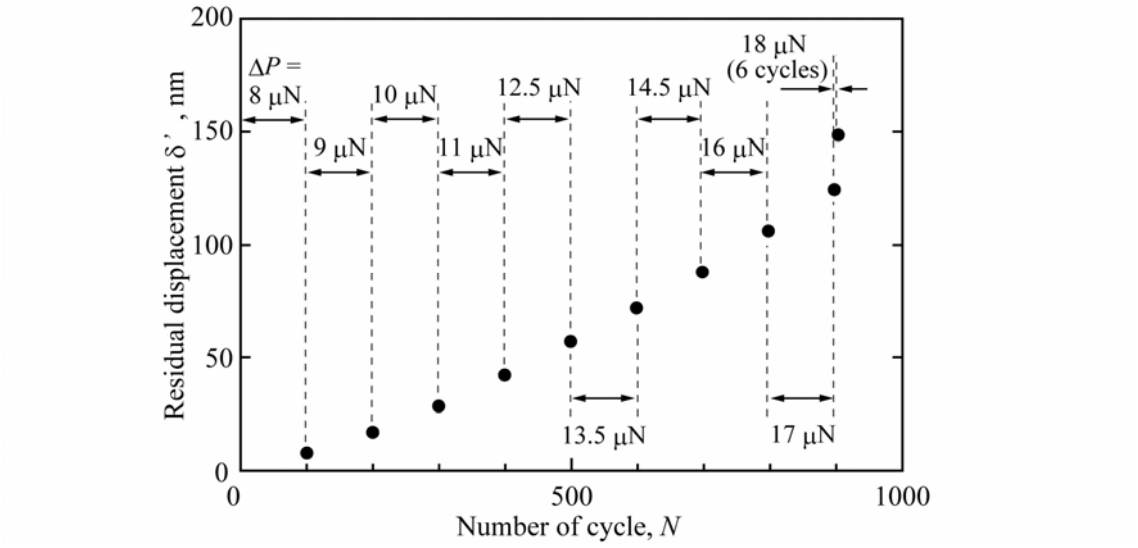

Fig.7 Residual displacement, δ', with respect to the number of cycles, *N*.

3.2 Fatigue fracture

Figure 8(a) shows the load-time (*P*-*t*) relationship under ΔP = 18 μN where the specimen breaks in the 7th cycle. The specimen is cyclically loaded until the 6th cycle without any damage observed on the interface. In the 7th cycle, the load suddenly drops before the maximum load (17.0 μN; point E in Fig. 8(a)), and the specimen breaks along the Cu/Si interface. Since the load at E is about 6 % smaller than P_{max} = 18 μN, it is clearly different from the fracture in monotonic loading. The TEM micrographs in Fig. 8(b) show that there is no remarkable damage in the Cu/Si interface in the specimen

京都大学 KYOTO UNIVERSITY
A Self-archived copy in
Kyoto University Research Information Repository
https://repository.kulib.kyoto-u.ac.jp
京都大学学術情報リポジトリ KURENAI 紅 Kyoto University Research Information Repository

before the break.

Figure 9 shows the *P*-δ curve for each cycle. The nonlinear behavior and distinct hysteresis loop indicate the cyclic plasticity of the Cu film because the Si substrate and the SiN layer are elastically deformed at this load level. After the 2nd cycle, reverse yielding appears during the unloading process. These suggest the development of a cyclic substructure in the Cu film.

As shown in Fig.7, the residual displacement increases rapidly after the load range is increased to ΔP = 18 μN. The average in one cycle is 4.0 nm, which is more than one-order larger than that under ΔP = 17 μN. This drastic softening of the Cu film may also be due to the transition and development of the cyclic substructure. The width of the cyclic *P*-δ curve becomes narrower with increasing number of fatigue cycles. Figure 10 shows the half bandwidth of the cyclic loop, $w_{1/2}$, with respect to the number of cycles. $w_{1/2}$ gradually decreases with the progress of cyclic deformation, and the magnitude in the 6th cycle is about half of that in the 1st cycle. This indicates cyclic hardening in the Cu film owing to the transition of the substructure.

京都大学 KYOTO UNIVERSITY
A Self-archived copy in
Kyoto University Research Information Repository
https://repository.kulib.kyoto-u.ac.jp
京都大学学術情報リポジトリ KURENAI 紅 Kyoto University Research Information Repository

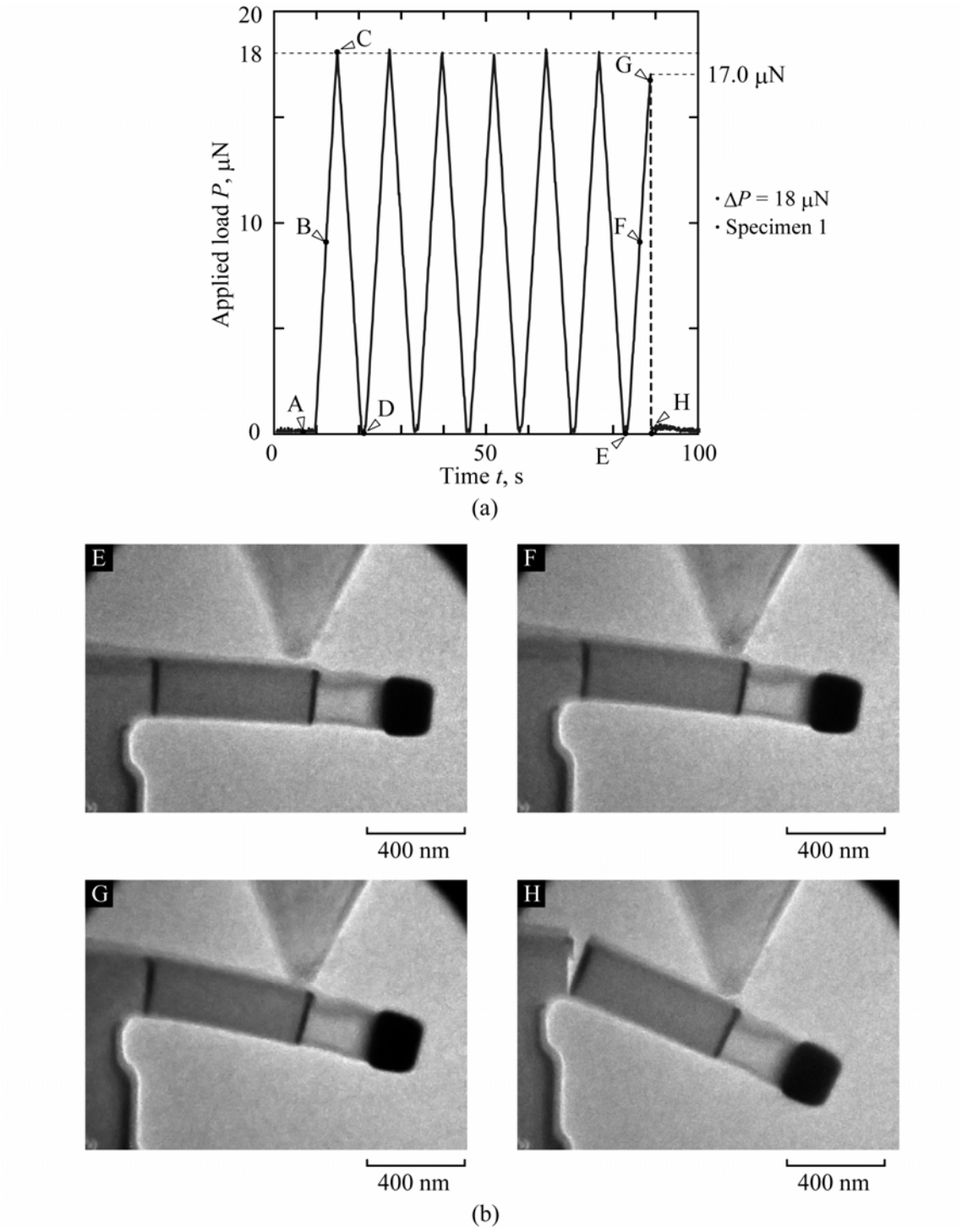

Fig. 8 (a) Load-time relationship under the load range of 18 μN, and (b) TEM micrographs when the specimen breaks.

京都大学 KYOTO UNIVERSITY
A Self-archived copy in
Kyoto University Research Information Repository
https://repository.kulib.kyoto-u.ac.jp
京都大学学術情報リポジトリ KURENAI 紅 Kyoto University Research Information Repository

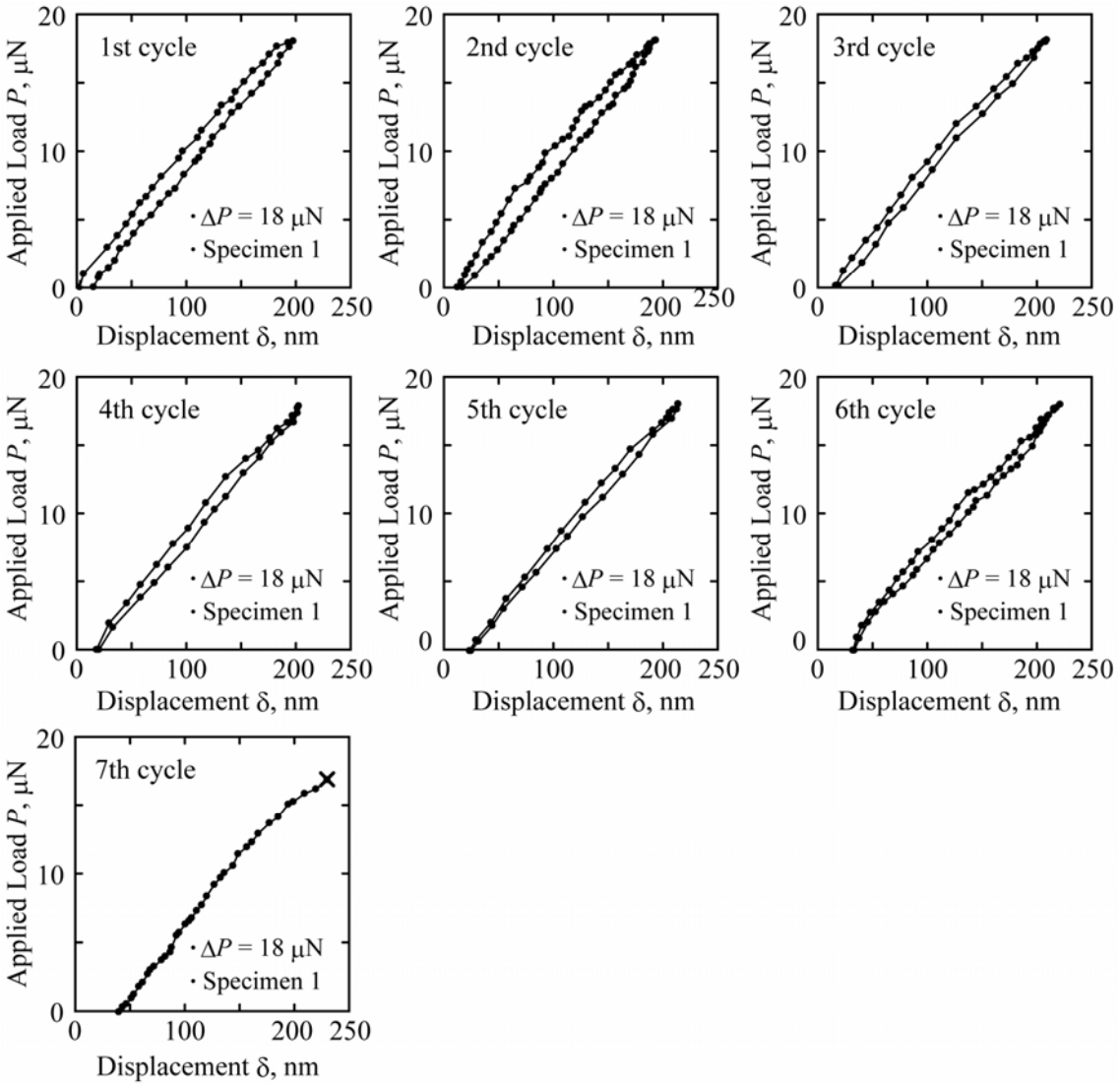

Fig. 9 Load-displacement curves under the load range of 18 μN.

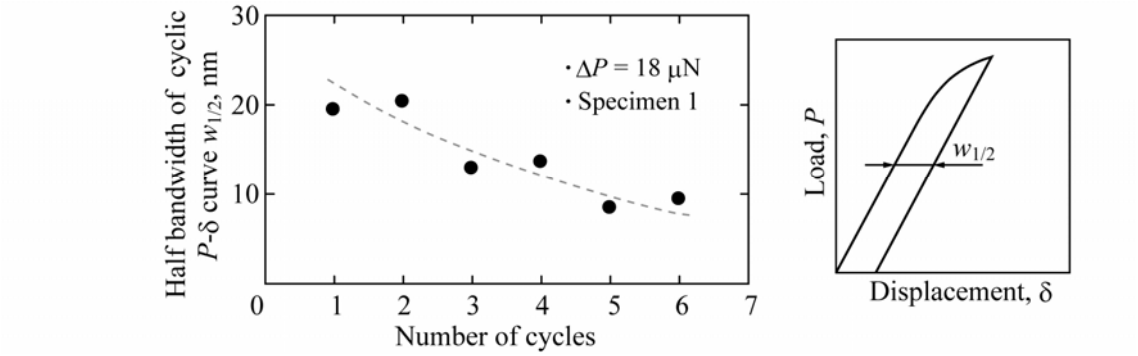

Fig. 10 Change of half bandwidth of the *P*-δ loop under the load range of 18 μN.

京都大学 KYOTO UNIVERSITY
A Self-archived copy in
Kyoto University Research Information Repository
https://repository.kulib.kyoto-u.ac.jp
京都大学学術情報リポジトリ KURENAI 紅 Kyoto University Research Information Repository

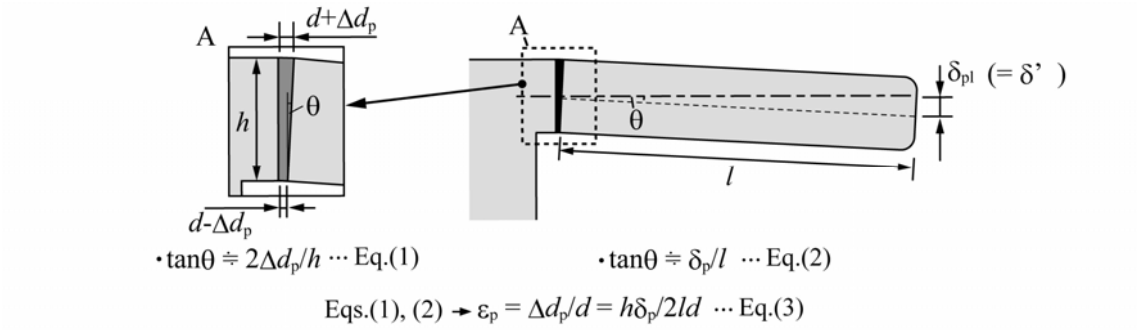

Fig. 11 Geometric relationship between the plastic strain of the Cu film, ε_p and the residual plastic displacement of the arm end, δ_p.

3.3 Cumulative plastic strain

Since the formation of a cyclic substructure can sustain a large cumulative plastic strain, the cumulative plastic strain of the Cu film until fracture is approximately estimated and is compared with that in the monotonic bending experiment. The plastic strain is calculated from the residual displacement of cantilever, δ', (See Fig. 11) at the null load.

Let us assume plastic stretching of Cu thickness on the top and the bottom surfaces at $P = 0$ of Δd_p and $-\Delta d_p$, respectively. Using the inclination angle of the cantilever, θ, we have:

$$\tan\theta \approx 2\Delta d_p / h, \tag{2}$$

where h is the height of the cantilever. On the other hand, tan θ is related to δ_p as:

$$\tan\theta \approx \delta_p / l. \tag{3}$$

where l is the distance from the Cu/Si interface to the arm end. From Eqs. (2) and (3), the plastic strain on the upper surface of the Cu film, ε_p, is given by:

$$\varepsilon_p = \frac{\Delta d_p}{d} \approx \frac{h\delta_p}{2ld}. \tag{4}$$

where d is the thickness of the Cu film. Inserting δ_p = 148 nm, which is the residual displacement observed at fracture, ε_p is evaluated to be 0.87.

Figure 12 shows the P-δ curve in the monotonic loading of Specimen 2, wherein the relation derived from elastic FEM analysis is superimposed using a solid line. The plastic displacement at fracture, δ_p, is about 50 nm, and this approximately gives a fracture strain of 0.23. The accumulated strain under fatigue is more than three times larger than that under monotonic loading. In fatigue of bulk metals, characteristic dislocation structures (e.g. ladder like structure and cell structure) are formed while

京都大学 KYOTO UNIVERSITY
A Self-archived copy in
Kyoto University Research Information Repository
https://repository.kulib.kyoto-u.ac.jp
京都大学学術情報リポジトリ KURENAI 紅 Kyoto University Research Information Repository

monotonic loading brings about rather simple structure. The structure in fatigue carries larger cumulative plastic strain. Thus, our experimental results suggest that the Specimen 1 breaks owing to the characteristic fatigue microstructure in nanometer scale due to cyclic plasticity, though elucidation of the detailed morphology is left to future work.

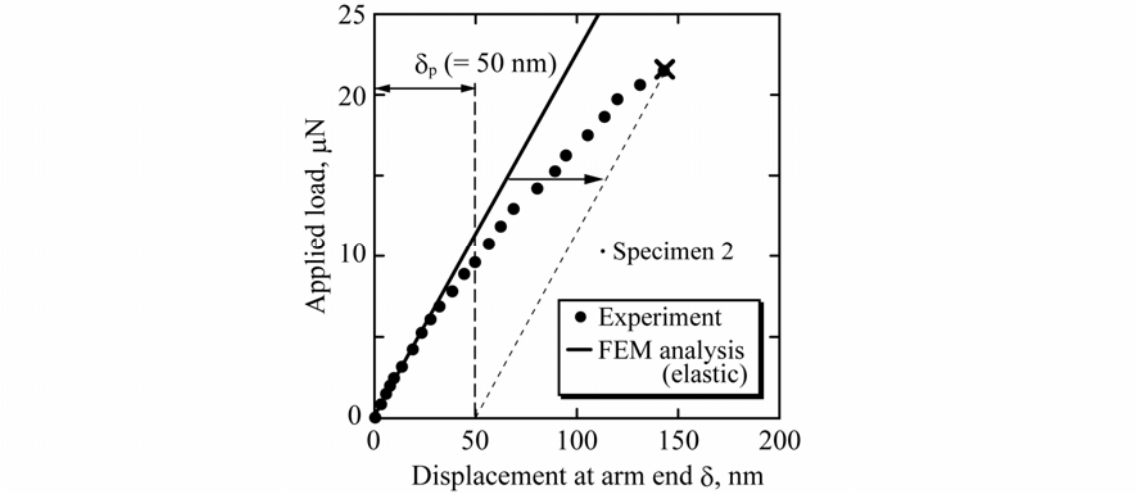

Fig. 12 Load-displacement curve in monotonic loading of Specimen 2.

4 Conclusions

In order to examine fatigue in a nanoscale region, a cyclic bending experiment was conducted using a nano-component specimen wherein a 20 nm-thick Cu film was sandwiched by a Si substrate and a SiN layer. The results can be summarized as follows.

(1) The specimen, which possesses a fatigue (high strain) region of about 40 nm×20 nm×330 nm in the Cu film, breaks in the 7th cycle under a load range of 18.0 μN. The fracture load (P = 17.0 μN) was 6 % smaller than the maximum load.

(2) The cyclic load-displacement curve shows distinct hysteresis due to the cyclic plastic deformation of the Cu film. Moreover, the decrease in the P-δ curve width with the progress of cyclic deformation indicates cyclic hardening of the Cu film. This suggests the development of a cyclic substructure in the Cu film.

(3) The cumulative plastic strain of the Cu film at fracture is approximately evaluated to be 0.87, which is more than three times larger than for monotonic loading (= 0.23). This result indicates that the specimen breaks owing to the characteristic fatigue substructure developed in the Cu film.

京都大学 KYOTO UNIVERSITY
A Self-archived copy in
Kyoto University Research Information Repository
https://repository.kulib.kyoto-u.ac.jp
京都大学学術情報リポジトリ KURENAI 紅 Kyoto University Research Information Repository

Acknowledgments

This work was supported in part by a Grant-in-Aid for Scientific Research (S)(No.21226005), of the Japan Society for the Promotion of Science, and by a Grant-in-Aid for Young Scientists (A)(No. 21686013) from the Ministry of Education, Culture, Sports, Science and Technology, Japan.

京都大学 KYOTO UNIVERSITY
A Self-archived copy in
Kyoto University Research Information Repository
https://repository.kulib.kyoto-u.ac.jp
京都大学学術情報リポジトリ KURENAI 紅 Kyoto University Research Information Repository

References

[1] Mughrabi H, Mater. Sci. and Eng. 1978;33:207-23.
[2] Essmann U, Gosele U, Mughrabi H Phil.Mag. A 1981;44:405-26.
[3] Laird C, Charsley P, Mughrabi H, Mater. Sci. and Eng. 1986;81:433-50.
[4] Finney J M, Laird C Phil. Mag. 1975;31:339-66.
[5] Winter A T, Phil. Mag., 1974;30(4):719-738.
[6] Kuhlmannwilsdorf D, Laird C Mater. Sci. and Eng. 1977;27:137-56.
[7] Kuhlmannwilsdorf D, Laird C, Mater. Sci. and Eng., 1980;46:209-19.
[8] Liu W, Bayerlein M, Mughrabi H, Acta Metall. 1992;40(7):1763-71.
[9] Polak J, Liskutin P Fatigue Fract. Eng. Mater. Struct. 1990;13:119-33.
[10] Lim LC Acta Metall. 1987;35:1653-62.
[11] Bogy DB J Appl. Mech. 1968;35:460-6.
[12] Bogy DB J Appl. Mech. 1971;38:377-86.
[13] Sun XJ, Wang CC, Zhang J, Liu G, Zhang GJ, Ding XD, Zang GP, and Sun J J Phys. D 2008;41:195404-1-6.
[14] Niu RM, Liu G, Wng C, Zhang G, Ding XD, and Sun J Appl. Phys. Lett. 2007;90:161907-1-3.
[15] Zhang GP, Sun KH, Zhang B, Gong J, Sun C, Wang ZG Mater. Sci. Eng., A 2008;483-484:397-90.
[16] Hirakata H, Takahashi Y, Van Truong, Kitamura T. Int. J. Fract. 2007;145(4):261-71.
[17] Hirakata H, Hirako T, Takahashi Y, Matsuoka Y, Kitamura T Eng. Frac. Mech. 2008;75(10):2907-20.
[18] Sumigawa T, Shishido T, Murakami T, Kitamura T Mater. Sci. & Eng. A, 2010;527:4796-803.
[19] Sumigawa T, Hirakata H, Takemura M, Matsumoto S, Suzuki M, Kitamura T Eng. Frac. Mech. 2008;75(10):3073-83.
[20] Takahashi Y, Hirakata H, aKitamura T Thin Solid Films 2008;516:1925-30.
[21] Sumigawa T, Shishido T, Murakami T, Iwasaki T, Kitamura T Thin Solid Films, submitted.
[22] Nix WD, Metall. Mater. Trans. 1989;20:2217-14.
[23] ASM Handbook, Mechanical Testing and Evaluation, 2000;8.